Medium-energy ion-scattering study of strained holmium silicide nanoislands grown on silicon (100)

T. J. Wood,[1] C. Eames,[1] C. Bonet,[1] M. B. Reakes,[1] T. C. Q. Noakes,[2] P. Bailey,[2] and S. P. Tear[1,*]
[1]*Department of Physics, University of York, Heslington, York, YO10 5DD, United Kingdom*
[2]*STFC Daresbury Laboratory, Daresbury, Warrington, WA4 4AD, United Kingdom*
(Received 9 April 2008; revised manuscript received 11 June 2008; published 15 July 2008)

We have used medium-energy ion scattering (MEIS) to quantitatively analyze the structure of holmium silicide islands grown on the Si(100) surface. Structure fitting to the experimental data unambiguously shows that the tetragonal silicide phase is present and not the hexagonal phase, which is associated with the growth of nanowires at submonolayer coverages. Islands formed with a lower holmium coverage of 3 ML are also shown to be tetragonal, which suggests that the hexagonal structure is not a low coverage precursor to the growth of the tetragonal phase. MEIS simulations of large nanoislands, which include the effects of lateral strain relief, have been performed and these compare well with the experimental data.

DOI: 10.1103/PhysRevB.78.035423 PACS number(s): 61.46.−w, 61.43.Bn, 61.05.Np

I. INTRODUCTION

While there have been many studies of rare-earth (RE) silicides on the Si(111) surface, relatively little was known about the growth mechanisms on the Si(100) surface until the discovery of self-assembled nanowires by Preinesberger *et al.*[1] These structures form when a suitable RE metal, e.g., Gd,[2–6] Sc,[4] Dy,[1,7–10] Sm,[4] Er,[7,8,11–13] Ho,[8,14] or Y,[15] is deposited onto a clean Si(100) substrate held at an elevated temperature. Characteristic "wires" measuring up to a micrometer in length and typically only a few nanometers wide were observed by scanning tunneling microscopy (STM). This discovery and the potential technological applications of such conducting nanowires have motivated considerable interest over the last ten years.[2–28] Chen *et al.*[11] have demonstrated that the growth of nanowires with extremely high aspect ratios is the result of the anisotropic lattice mismatch that results from the growth of the hexagonal, defect-AlB_2 RE silicide on the Si(100) surface (see Fig. 1).

Depositing more RE metal causes islands to form with the surface displaying a c(2×2) periodicity. The structure of these RE silicide islands has been proposed to be either hexagonal, tetragonal ($ThSi_2$), or orthorhombic ($GdSi_2$).[1,6,10,12,13,16,17,22,27,28] All three of these phases are known to exist in the bulk and their lattice constants have been measured, and it is known that the bulk orthorhombic phase is only a small distortion of the tetragonal phase.[29] A side-view schematic of the $ThSi_2$ structure is shown in Fig. 2. Evidence for the growth of the tetragonal form has generally been inferred from lattice mismatch arguments along with STM measurements of step heights in the silicides on the Si(100) surface.[13] Surface x-ray diffraction (SXRD) measurements also yield information, which appears to confirm that Er silicide islands adopt the tetragonal form, with the surface c(2×2) periodicity interpreted as being due to Si adatoms.[12]

STM experiments reveal that the island morphology is very sensitive to the RE metal deposited and to the annealing temperature used. Those RE metals (Nd, Sm, and Yb) that have a low anisotropy in their lattice match to the substrate form compact three-dimensional (3D) islands.[8] Those that have a high anisotropy form both elongated and compact islands, depending upon the growth temperature. Growth at lower temperatures (600 °C) causes the formation of elongated islands and growth at temperatures above 650 °C results in compact 3D islands. However, the two island morphologies have been observed to coexist, especially when using intermediate annealing conditions.

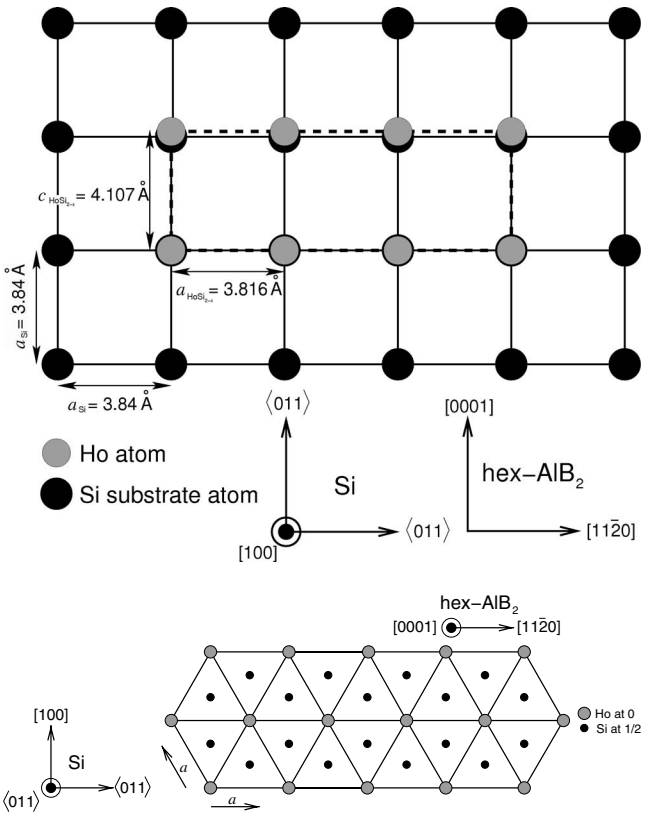

FIG. 1. (a) A top down schematic illustrating the lattice matching of the hexagonal defect-AlB_2 structure to the Si(100) surface. The anisotropy in lattice mismatch creates the high aspect ratio nanowires commonly observed for several RE metals. (b) A side-view schematic of the AlB_2 structure.

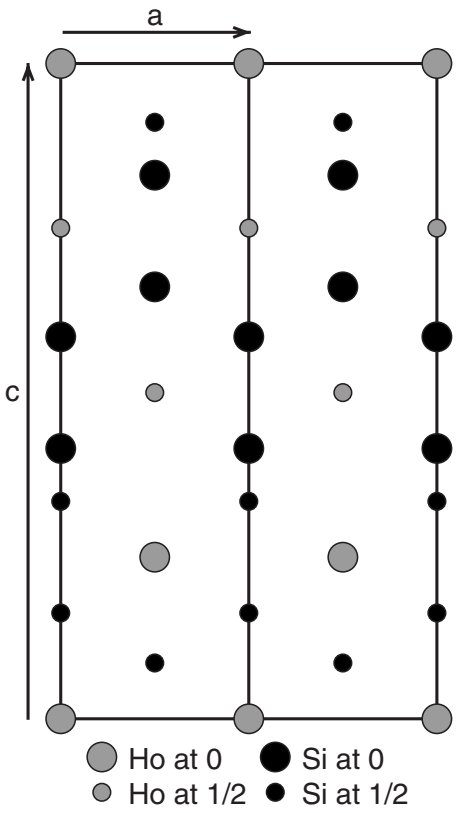

FIG. 2. A side-view schematic of the tetragonal $ThSi_2$ structure. The orthorhombic $GdSi_2$ structure of $HoSi_2$ is essentially the same but with $a=4.03$ Å and $b=3.94$ Å, a difference of just 2.25%.

Dysprosium silicide provides an interesting case study. The elongated islands have typical dimensions 2 nm high, 15 nm wide, and 500 nm long, and the smaller compact islands have typical dimensions 5 nm high, 50 nm wide, and 200 nm long.[22] Using high-resolution cross-sectional transmission electron microscopy (TEM), Ye *et al.*[27] demonstrated that elongated and nonelongated islands coexist when Dy silicide is grown at 600–650 °C on the Si(100) surface. They proposed that the structure of the elongated islands was hexagonal, and the excessive stress within this structure (due to the large *c*-axis mismatch) is relieved through dislocations and tilting across the width of the island. The nonelongated islands were found to be a tetragonal or orthorhombic structure with only a small amount of tilting required to relieve the stress since the lattice match is relatively small in both directions. It was also noted that there was some expansion of the *c* axis to relieve the stress in much the same way as has been demonstrated for the two-dimensional (2D) and 3D RE silicides on Si(111).[30,31] However, the recent high-resolution transmission electron microscopy (HRTEM) study by He *et al.*[22] claims that the compact 3D Dy silicide islands are in fact a fully relaxed, and hence stress free, hexagonal form while the elongated nanowire islands are tetragonal/orthorhombic with the faulted stacking relieving the stress in the structure. The delicate energy balance within the silicide in this particular example is also highlighted by the fact that there is both a tetragonal and an orthorhombic phase of Dy silicide in the bulk.

Despite the many studies that have been conducted, it has been noted in recent work that no ideal crystallographic determination has been possible to clearly prove once and for all the true nature of the 3D islands[22,26,28] created when the rare-earth metals form a silicide in this way. Medium-energy ion scattering (MEIS) is of particular value in the study of these nanostructures since the large mass contrast of Ho and Si allows the elucidation of the silicide structure free from substrate effects. This also means that the technique is able to isolate the regions of interest on the surface by only selecting the Ho signal for the structural optimization.

II. EXPERIMENT

All MEIS data were obtained at the UK MEIS facility at STFC Daresbury Laboratory. The experiments were conducted under ultrahigh vacuum (UHV) with typical base pressures of 2×10^{-10} mbar. Clean Si(100) samples (cut from a lightly doped *n*-type wafer) were prepared by *e*-beam heating to ~1200 °C for 1 min then slowly cooled (<100 °C min^{-1}) between 1000 and 600 °C, ensuring that an ordered surface was obtained. Temperature measurements were made using an infrared pyrometer. The heating cycles were repeated until a sharp 2×1 low-energy electron-diffraction (LEED) pattern was observed. The 3D silicide islands were then formed by depositing approximately 6 ML of Ho from a quartz-crystal calibrated tantalum boat source onto this clean Si(100) surface, which was held at ~650 °C during deposition and for 5 min afterward. When a $c(2\times2)$ LEED pattern was observed and the Auger-electron spectrum showed the samples to be free from contamination, they were transferred under UHV into the ion-scattering chamber.

The ion-scattering data were taken using 100 keV H^+ ions incident upon the sample, and the scattered ions were detected using an angle-resolving toroidal-sector electrostatic ion-energy analyzer and its microchannel plate detector. The MEIS spectra confirmed that the samples were free of contaminants and data were acquired with a total dose of $\sim10^{16}$ ions cm^{-2}. Further details about the Daresbury MEIS facility can be found in the literature.[30,32–35] During each experiment two different incident-beam directions onto the sample were used. These beam directions are shown with respect to the substrate in Fig. 3. The notation $[in]/[out]$ for each geometry defines the ingoing crystal direction $[in]$ and an outgoing crystal direction $[out]$ that lies in the detected angular range of the scattered ions.

III. STRUCTURE FITTING: TETRAGONAL OR HEXAGONAL?

Due to the contention in the literature regarding whether these islands take the hexagonal, tetragonal, or orthorhombic form, MEIS proves particularly powerful since it can clearly demonstrate the presence of one of these structures. In this work we have used the XVEGAS code,[36] which uses Monte Carlo methods to simulate the blocking curves of a proposed structural model.

Figure 4(a) shows the simulated blocking curves obtained when differing numbers of layers of RE are present in the hexagonal structure for the $[\bar{1}\bar{1}0]/[1\bar{1}0]$ geometry. The interlayer separation of all the Ho layers has been optimized to

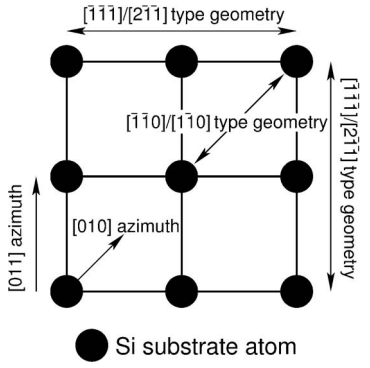

FIG. 3. View from above of the bulk terminated Si(100) surface showing the two incident-beam directions used in the MEIS experiments. For the $[\bar{1}\bar{1}0]/[1\bar{1}0]$ geometry, the angle with respect to the sample normal was 45° and for the $[\bar{1}\bar{1}\bar{1}]/[2\bar{1}\bar{1}]$ geometry, the polar angle was 54.74°. The scattering plane through the tetragonal silicide is shown for the $[\bar{1}\bar{1}0]/[1\bar{1}0]$ geometry in Fig. 9.

give the best visual agreement with experimental data with the two intermediate Si layers lying one third and two thirds of this layer separation from the Ho layer beneath. A Ho-Ho layer separation of 3.28 Å has been found to give the best fit. However, the quality of the fits obtained is very poor, clearly demonstrating that this is not the correct structure. To make this clearer, the fit for six layers of Ho is shown in Fig. 4(b). At scattering angles of 88°, 90°, 100°, 106°, 118°, 127°, and 142°, there are major discrepancies between the experimental data and the best-fit simulations. The fully relaxed hexagonal structure that was proposed by He *et al.*[22] does not explain the experimental blocking curves either; as such a structure would produce almost identical blocking curves but would yield a smaller *c*-axis of the silicide.

The tetragonal structure has also been fitted to the data since it is assumed that the silicide takes the same *a* and *b* values as the Si substrate to form an epitaxial overlayer. This goes against the available data in the literature regarding the structure of the *bulk* Ho silicides as no tetragonal phase has been observed (although the orthorhombic $GdSi_2$ form has been reported with lattice parameters of $a=4.03$ Å, $b=3.944$ Å, and $c=13.30$ Å).[29] Conducting simulations of such a tetragonal structure gives the fits for the $[\bar{1}\bar{1}0]/[1\bar{1}0]$ geometry shown in Fig. 5(a), which are for structures that are one, two, and three $ThSi_2$-type cells in height. It is clear that a crystal with a depth of two $ThSi_2$ cells produces the best match. The detailed structure fits are shown in Figs. 5(b) and 5(c). The rms thermal vibrations of the Ho atoms were set to the bulk metal value of 0.13 Å while a fitting of the Si vibrations gives an enhanced value of 0.15 Å. These vibrations are consistent with the previous MEIS studies of 2D and 3D RE silicides on Si(111) (Refs. 31 and 35) with the factor of two enhancement for the Si atoms possibly indicating the presence of static disorder in these layers. This could be due to the presence of Si vacancies.[20,25]

Optimizing the layer separation of the Ho atoms gives the best visual agreement for both geometries when $c=13.14$ Å. It is clear from comparing Fig. 5(b) with Fig. 4(b) that the tetragonal form of the silicide is a better fit to the data than the hexagonal structure.

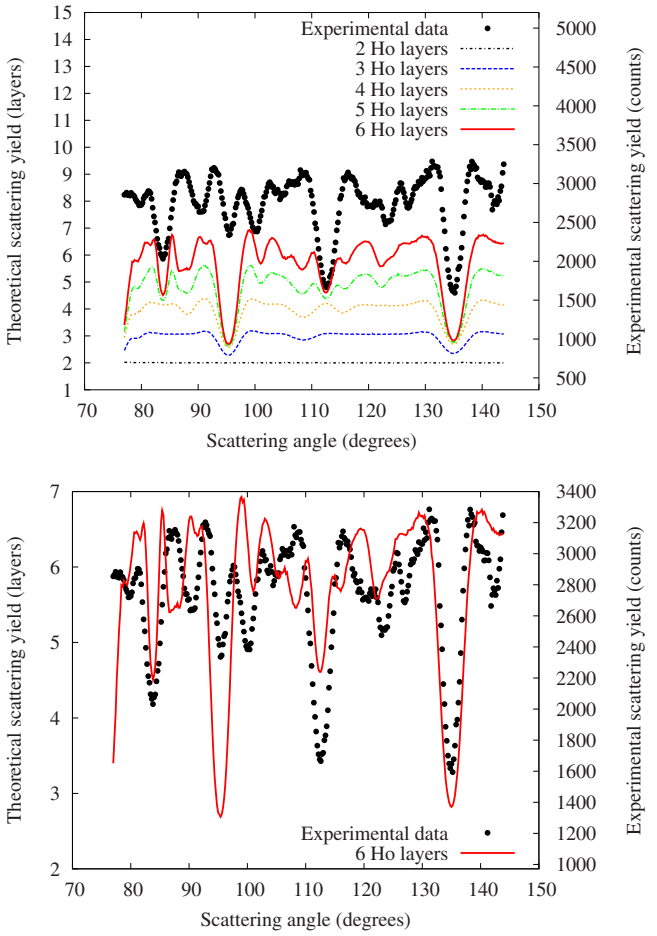

FIG. 4. (Color online) (a) A comparison of the simulations of the hexagonal structure with two to six layers of Ho to the experimental data for the $[\bar{1}\bar{1}0]/[1\bar{1}0]$ geometry. (b) The fit obtained for six Ho layers in the hexagonal structure with a Ho-Ho layer separation of 3.28 Å.

IV. ANOMALOUS *c*-AXIS VALUE

The assumption that the silicide grows epitaxially on the Si(100) surface yields a constant *c*-axis value throughout this silicide (13.14 Å) that is much smaller than the value of 13.30 Å for the bulk silicide. We expect that the stress induced through a contraction of the Ho silicide *a* and *b* axes at the interface would be released through an expansion in the perpendicular direction, and such behavior has been directly observed in other rare-earth silicide surfaces.[30,31] In particular, Ye *et al.*[27] have reported an expansion in the *c* axis of the silicide relative to the bulk value for Dy on Si(100).

One explanation for this observation could be that the silicide is incommensurate with the Si substrate. Hence it would seem reasonable to assume that the silicide takes the orthorhombic form that is observed for bulk Ho silicide. Refitting the experimental data to simulations of this structure, where $a=4.030$ Å and $b=3.944$ Å, yields almost identical fits but with a *c* axis of 13.70 Å. This large value of the silicide *c* axis does not make sense according to the established trend in strain either, as it would be expected that the lack of strain at the interface would not cause any expansion

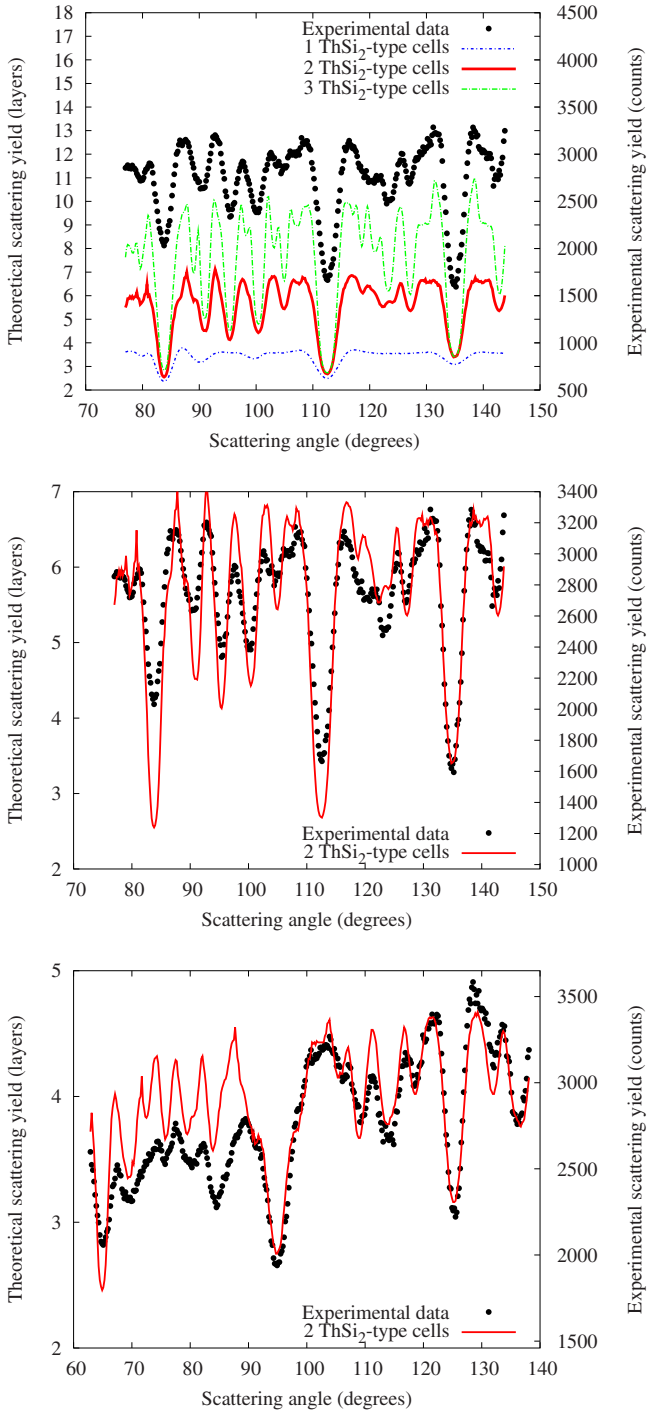

FIG. 5. (Color online) (a) Comparison of simulations of the tetragonal structure with thicknesses of two to four $ThSi_2$ cells in height to the experimental data for the $[\bar{1}\bar{1}0]/[1\bar{1}0]$ geometry. (b) The fit obtained for the $[\bar{1}\bar{1}0]/[1\bar{1}0]$ geometry when the silicide is two $ThSi_2$ cells in height. (c) The fit obtained for the $[\bar{1}\bar{1}\bar{1}]/[2\bar{1}\bar{1}]$ geometry when the silicide is two $ThSi_2$ cells in height.

in the c axis of the silicide relative to the bulk value. Thus it can be concluded that it is not the bulk form of the silicide that is present on the surface; it must be some intermediate form.

TABLE I. Optimized c-axis values determined for various fixed values of the a axis. Fitting the $[\bar{1}\bar{1}0]/[1\bar{1}0]$ and $[\bar{1}\bar{1}\bar{1}]/[2\bar{1}\bar{1}]$ geometries yield slightly different values, which can be averaged to give an overall best-fit value.

a (Å)	c_{110} (± 0.04 Å)	c_{111} (± 0.04 Å)	c_{average} (± 0.04 Å)
3.84	13.12	13.16	13.14
3.88	13.24	13.28	13.26
3.92	13.40	13.44	13.42
3.96	13.52	13.56	13.54
4.00	13.68	13.72	13.70

One of the limitations of MEIS when only using the Ho blocking curves to solve crystallographic structure is that it is not possible to exclusively determine both the a and c axis lattice constants of the silicide. This is because any difference in the silicide a axis could be compensated by a change in the c axis to produce blocking curves with blocking dips in the same positions. Hence, a particular c/a ratio will yield a series of blocking curves that are exactly the same even though the actual lattice parameters may be very different. We have performed a series of simulations, each with a fixed a axis, in which the c axis has been optimized by varying the layer separation of a silicide that is two $ThSi_2$ cells in height. These results are shown in Table I.

The data from Table I are plotted in Fig. 6 and the straight-line fit defines a c/a ratio of 3.42 ± 0.01. The positive gradient suggests that as the lateral lattice constant of the tetragonal unit cell is reduced to match that of the substrate, the lattice constant perpendicular to the surface also contracts, and this is true for all pairs of c and a values. As noted earlier, we might expect the opposite to occur and the c axis to expand in order to maintain the volume of the unit cell.

V. SIMULATION OF STRAINED ISLANDS

There is another reason that might explain the unusually low c axis suggested by the fitting procedure. If the lateral

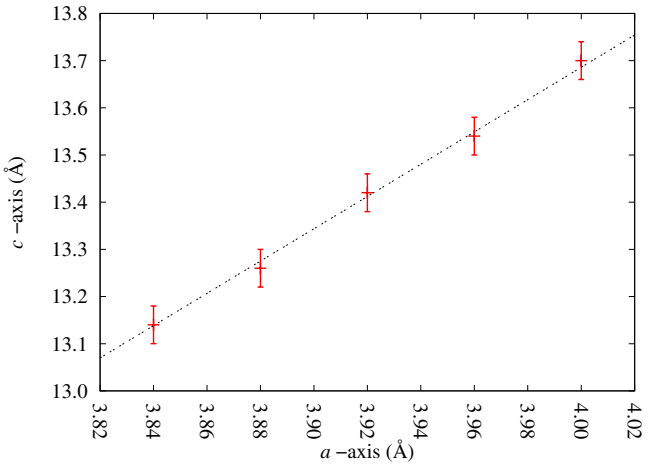

FIG. 6. (Color online) A plot showing how the determined c axis is dependent on the size of the a axis of the silicide. Fitting a straight line that passes through the origin yields a c/a ratio of 3.42 ± 0.01.

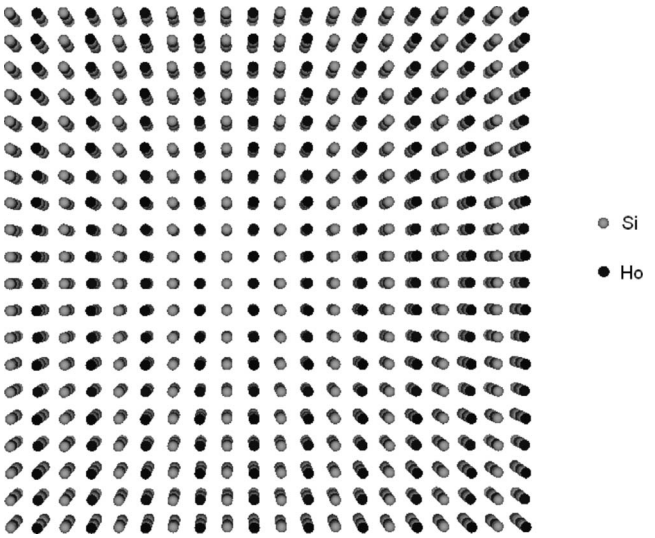

FIG. 7. View from above of the $10\times10\times2$ unit cell showing the lateral strain.

lattice constant of the unit cell is constrained to match that of the substrate at the interface and is allowed to expand to relieve strain as we move away from the interface then the blocking angles will be shifted. The average a axis throughout the structure will increase and so will the fitted c axis in order to maintain the c/a ratio of 3.42. This effect would allow for interfacial matching and would, at the same time, provide a more physically meaningful thickness for the silicide.

Simulation of this effect is computationally intensive. Unit cells with lateral strain as a function of height do not laterally tessellate *ad infinitum* and a structure with finite lateral extent must be considered. This must be large enough to approach the size of a typical surface island but small enough to be computationally tractable. We have taken a unit cell with a 10×10 lateral extent, making an island 38.4×38.4 Å^2. This is two tetragonal unit cells deep and in total includes 2500 atoms. Computational resources prohibit us from a full optimization of the strained structure in terms of interlayer spacings or vibrational amplitudes. Instead we have taken values suggested from the structure fitting carried out on the $1\times1\times2$ cells detailed earlier in this work. The lateral lattice constants are allowed to relax from a value of 3.84 Å at the bottom of the supercell [interfacial matching to Si(100)] to 3.99 Å at the top of the supercell (the averaged unstrained lateral lattice constant of bulk orthorhombic holmium silicide). The strain relief is just a linear function of height and, for example, we have not considered a case in which only the few layers near the interface are significantly strained. The strained island from above is shown in Fig. 7.

Since we cannot currently fully optimize the c axis in such a strained island, we have simulated the blocking curves for four such islands, each with a different depth. This depth is varied by choosing two different c axes for the two unit cells that form the island. These four c axis values are: (1) both as bulk c axis values (13.30 Å), (2) both at the values obtained earlier in structure fitting with $1\times1\times2$ cells with no strain relief (13.14 Å), (3) expansion of the c axis of

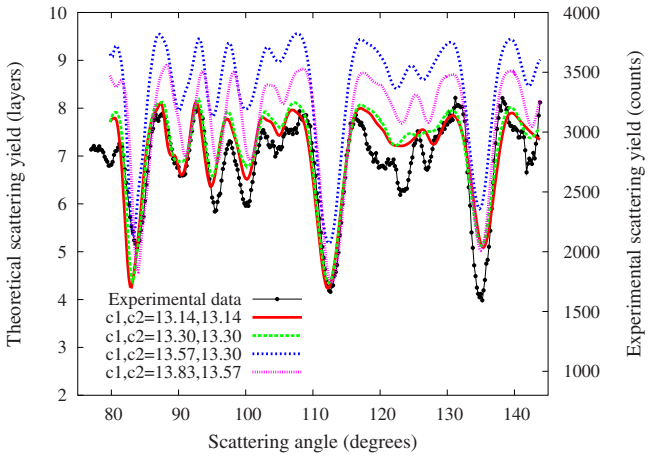

FIG. 8. (Color online) Comparison of simulated strain in large $10\times10\times2$ unit cells with experiment. The lateral lattice constant of each unit cell that makes up the nanoisland was allowed to relax from 3.84 Å [interface lattice matching with Si(100)] to 3.99 Å on the surface (bulk lattice constant). The four simulations plotted here correspond to fixed values of the two c axes in the $10\times10\times2$ unit cell. The first unit cell ($c1$) is nearest the surface and the second ($c2$) is nearest the interface.

the cell nearest the interface by 2% and a bulk c axis value in the top unit cell (13.57 and 13.30 Å), and (4) expansion of the c axis of the cell nearest the interface by 4% and the top cell by 2% (13.83 and 13.57 Å). The calculated blocking curves are shown in Fig. 8 for the $[\bar{1}\bar{1}0]/[1\bar{1}0]$ geometry, the $[\bar{1}\bar{1}\bar{1}]/[2\bar{1}\bar{1}]$ geometry not being calculated because it would require averaging over two possible domains and thus use twice as many simulations.

On first viewing, the incorporation of strain appears to make the fit worse [compare with the fit for the $1\times1\times2$ cell in Fig. 4(b)]. The region with a scattering angle in the approximate range $117°-129°$ is especially bad. The scattering plane is shown schematically in Fig. 9. We can see from this that in the regions where the fit is bad, it is the positions of the silicon atoms that are responsible for the poor fit of the

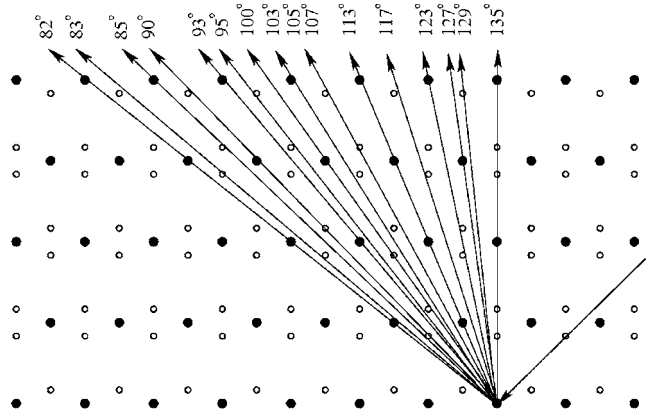

FIG. 9. Schematic slice showing the scattering plane for the $[\bar{1}\bar{1}0]/[1\bar{1}0]$ geometry and the atoms responsible for the principal blocking dips observed. Filled circles represent Ho atoms and empty circles represent silicon atoms.

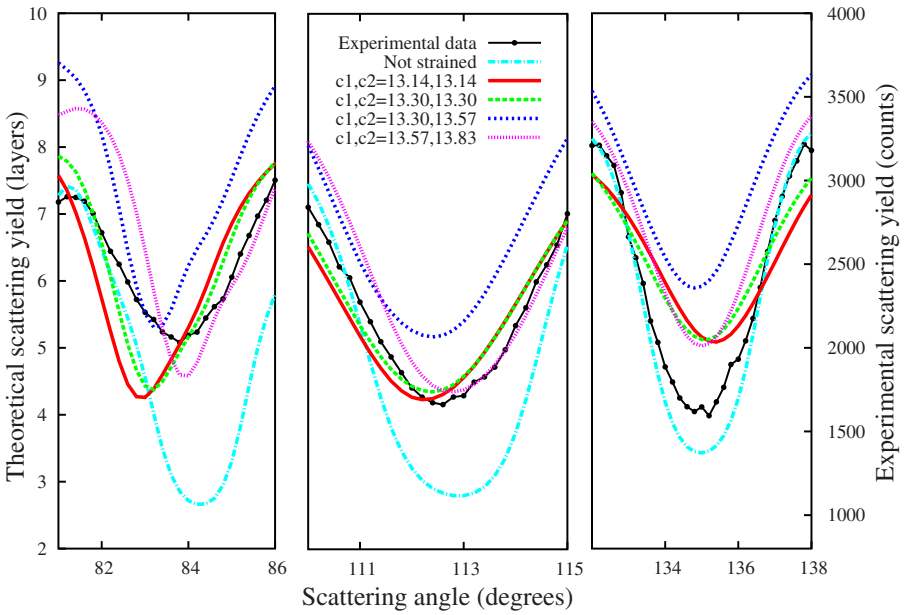

FIG. 10. (Color online) Showing the detail around the major blocking dips in Fig. 8. With the gradual introduction of larger, more physically reasonable *c*-axis values into the strained cells, the fit is improved until it is better than that for the fully optimized but nonstrained cell.

blocking dips. Another minor silicon atom blocking dip at around 107° is also a poor fit. Given that the positions and the thermal vibrations of the silicon atoms have not been optimized, it is no surprise that the fit is made worse by the introduction of strain.

However, the blocking dips produced by this structure are dominated by those caused by holmium atoms, and close inspection of the major blocking dips at roughly 82°, 113°, and 135° supports the possibility of strain in these structures. The detail around these blocking dips is shown in Fig. 10. In the strained cells as the *c* axes are changed from the unrealistically low value obtained in the fit on an unstrained cell (13.14 Å) through the bulk silicide value (13.30 Å) and into the two cases where the *c* axis is expanded, the blocking dip is shifted to become closer and closer to the experimentally measured dip. Indeed, at 84° and 113°, the blocking dip for the strained cells is a better fit to experiment than that for the unstrained, fully optimized, and multilayer averaged fit.

Thus far, the question of the surface termination has not been addressed. The unit cells involved in the simulations are holmium terminated, which is not physically reasonable. Also, the LEED pattern shows a c(2×2) periodicity, which is not accounted for in any of the simulated cells. We have attempted to investigate the surface termination but the simulated blocking curves show very little sensitivity to an extra layer of silicon atoms that form a surface termination. Other experiments that are more sensitive to the very top atomic layer may be better suited to resolving the issue of the surface termination (such as MEIS itself at normal incidence with 50 keV He^+ ions).

VI. LOWER COVERAGES

The work presented here suggests that at a coverage of 6 ML and under our preparation conditions, strained tetragonal silicide islands are formed when holmium is grown on Si(100). At lower coverages (<1 ML), nanowires form, which are believed to be related to the hexagonal structure. The question naturally arises as to what structure forms in the intermediate coverage regime. Does the tetragonal structure grow atop the hexagonal phase? Or is there a phase change at a certain minimum coverage that results in tetragonal rather than hexagonal growth? To attempt to answer these questions, we have taken experimental data at a coverage of 3 ML under the same growth conditions. Figure 11 shows these data from the 3 ML sample compared with that from the sample grown using 6 ML of holmium.

The principal blocking dips at 113° and 135° are present in both samples. In the 6 ML sample, there are blocking dips at 90°, 95°, and 100° that are not produced from the 3 ML sample. If we refer to Fig. 9 we can see that these blocking dips are produced by holmium atoms in the upper region of the structure. We would not expect to see these features in a thinner silicide layer. In the hexagonal structure, the domi-

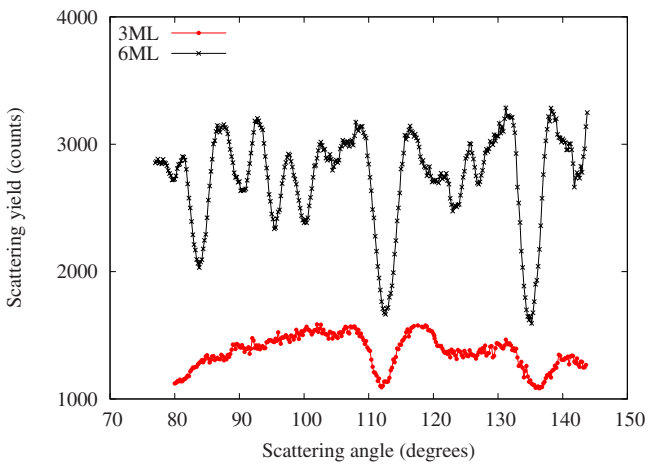

FIG. 11. (Color online) A comparison of the 6 ML coverage experimental data with data recorded after a sample was grown under identical growth conditions using a lower holmium coverage for the $[\bar{1}\bar{1}0]/[1\bar{1}0]$ geometry. The vertical scales have been artificially offset to aid the eye.

nant blocking dip is at a scattering angle of approximately 95° [see Fig. 4(a)]. The simulations suggest that this feature should be present in hexagonal silicides that contain as few as three layers of holmium. We can see no evidence for any blocking dips in this region in the experiment with 3 ML coverage and we must conclude that even at this coverage, the structure is tetragonal.

VII. SUMMARY AND CONCLUSION

Holmium silicide islands have been grown on the Si(100) surface and characterized using MEIS. Two structures have been fitted to the experimental data. This process clearly shows that under our growth conditions, it is the tetragonal phase of the silicide that is formed and not the hexagonal phase, and that these two structures do not coexist on the surface (the orthorhombic phase is too similar to the tetragonal phase for us to be able to determine if some of the orthorhombic nature of bulk HoSi is present in this surface tetragonal phase). A further experiment using a lower holmium coverage of 3 ML has also been shown to have the tetragonal structure, which confirms that the hexagonal phase is not the phase adopted at low coverages in this system.

Other authors have reported growth of the hexagonal phase under similar growth conditions for some of the other RE silicides. It is interesting to speculate as to why similar experiments have reached different structural conclusions. It would appear that the structure that is formed is very sensitive to the growth conditions. Island morphology is very sensitively dependent upon the particular RE metal deposited and the annealing temperature used. In the paper by He *et al.*,[22] they report a deposition rate of 0.5 ML per minute during the formation of $DySi_2$ whereas Ye *et al.*[27] report 0.3 ML per minute. It could be that the mobility of the RE metal and/or the lattice mismatch anisotropy of the particular silicide in question are important enough factors during the very early stages of silicide formation to dictate the final structure.

Using a simple $1\times1\times2$ tetragonal unit cell, the structure fitting suggests a *c* axis value that is too small to be physically reasonable when compared to the bulk structure. The blocking curves from a large 2500 atom $10\times10\times2$ nanoisland with lateral strain relaxation as a function of the distance from the interface have been simulated. The major blocking dips produced by this structure are a better fit to the experimental data than those produced by a nonstrained periodic structure. The lesser blocking dips produced by silicon atoms in the simulations do not show good agreement with experiment. This is to be expected because the thermal vibrations and the positions of these atoms have not been optimized in the structure fit. The results of the comparison of MEIS data with simulations clearly show that a physically reasonable *c* axis value for the holmium silicide can only be obtained if the islands are strained to fit the Si(100) at the interface and the strain allowed to relax toward the top of the islands.

A full structural fit for this system would require an optimization of the experiment-theory match with respect to all of the lateral and vertical spacings in the unit cell, and their variation with distance from the interface, taking into account lateral strain relief, vertical relaxation, and particular vibrations of each individual atom. This task is not currently tractable in terms of computational resources and the available computer codes.

ACKNOWLEDGMENTS

The authors would like to acknowledge the Engineering and Physical Science Research Council for funding this research. Paul Quinn and the FOM Institute are thanked for supplying the XVEGAS and VEGAS simulation codes. The assistance and technical support of Kevin Connell and Mark Pendleton are also much appreciated.

*spt1@york.ac.uk

[1] C. Preinesberger, S. Vandré, T. Kalka, and M. Dähne-Prietsch, J. Phys. D **31**, L43 (1998).
[2] A. Kirakosian, J. L. McChesney, R. Bennewitz, J. N. Crain, J.-L. Lin, and F. J. Himpsel, Surf. Sci. **498**, L109 (2002).
[3] J. L. McChesney, A. Kirakosian, R. Bennewitz, J. N. Crain, J. L. Lin, and F. J. Himpsel, Nanotechnology **13**, 545 (2002).
[4] Y. Chen, D. A. A. Ohlberg, and R. S. Williams, J. Appl. Phys. **91**, 3213 (2002).
[5] D. Lee and S. Kim, Appl. Phys. Lett. **82**, 2619 (2003).
[6] B. Z. Liu and J. Nogami, Nanotechnology **14**, 873 (2003).
[7] R. Ragan, Y. Chen, D. A. A. Ohlberg, G. Medeiros-Ribeiro, and R. S. Williams, J. Cryst. Growth **251**, 657 (2003).
[8] J. Nogami, B. Z. Liu, M. V. Katkov, C. Ohbuchi, and N. O. Birge, Phys. Rev. B **63**, 233305 (2001).
[9] B. Liu and J. Nogami, Surf. Sci. **488**, 399 (2001).
[10] B. Z. Liu and J. Nogami, J. Appl. Phys. **93**, 593 (2003).
[11] Y. Chen, D. A. A. Ohlberg, G. Medeiros-Ribeiro, Y. A. Chang, and R. S. Williams, Appl. Phys. Lett. **76**, 4004 (2000).
[12] G. Chen, J. Wan, J. Yang, X. Ding, L. Ye, and X. Wang, Surf. Sci. **513**, 203 (2002).
[13] Q. Cai and W. Zhou, J. Phys.: Condens. Matter **16**, 6835 (2004).
[14] C. Ohbuchi and J. Nogami, Phys. Rev. B **66**, 165323 (2002).
[15] M. Katkov and J. Nogami, Bull. Am. Phys. Soc. **47**, 283 (2002).
[16] N. Frangis, G. V. Tendeloo, J. V. Landuyt, G. Kaltsas, A. Travlos, and A. G. Nassiopoulos, Phys. Status Solidi A **158**, 107 (1996).
[17] N. Frangis, J. V. Landuyt, G. Kaltsas, A. Travlos, and A. G. Nassiopoulos, J. Cryst. Growth **172**, 175 (1997).
[18] J. C. Chen, G. H. Shen, and L. J. Chen, J. Appl. Phys. **84**, 6083 (1998).
[19] G. Chen, X. Ding, Z. Li, and X. Wang, J. Phys.: Condens. Matter **14**, 10075 (2002).
[20] K. S. Chi, W. C. Tsai, and L. J. Chen, J. Appl. Phys. **93**, 153 (2003).
[21] M. Kuzmin, P. Laukkanen, R. E. Perala, R. L. Vaara, and I. J. Varyrynen, Appl. Surf. Sci. **222**, 394 (2004).
[22] Z. He, D. J. Smith, and P. A. Bennett, Phys. Rev. B **70**, 241402(R) (2004).

[23] B. C. Harrison and J. J. Boland, Surf. Sci. **594**, 93 (2005).
[24] G. Pető, G. Molnár, Z. E. Horváth, C. S. Daróczi, E. Zsoldos, and J. Gyulai, Surf. Sci. **578**, 142 (2005).
[25] W. C. Tsai, H. C. Hsu, H. F. Hsu, and L. J. Chen, Appl. Surf. Sci. **244**, 115 (2005).
[26] L. Pasquali and S. Nannarone, Nucl. Instrum. Methods Phys. Res. B **230**, 340 (2005).
[27] G. Ye, J. Nogami, and M. A. Crimp, Thin Solid Films **497**, 48 (2006).
[28] G. Ye, M. A. Crimp, and J. Nogami, *Assembly at the Nanoscale-Toward Functional Nanostructured Materials*, MRS Symposia Procedings No. 901 (Materials Research Society, Pittsburgh, 2006), Paper No. Ra13.
[29] *Properties of Metal Silicides*, edited by K. Maex and M. V. Rossum (Institution of Engineering and Technology, Leuven, Belgium, 1995).
[30] C. Bonet, I. M. Scott, D. J. Spence, T. J. Wood, T. C. Q. Noakes, P. Bailey, and S. P. Tear, Phys. Rev. B **72**, 165407 (2005).
[31] T. J. Wood, C. Bonet, T. C. Q. Noakes, P. Bailey, and S. P. Tear, Phys. Rev. B **73**, 235405 (2006).
[32] D. J. Spence, S. P. Tear, T. C. Q. Noakes, and P. Bailey, Phys. Rev. B **61**, 5707 (2000).
[33] D. J. Spence, T. C. Q. Noakes, P. Bailey, and S. P. Tear, Surf. Sci. **512**, 61 (2002).
[34] D. J. Spence, T. C. Q. Noakes, P. Bailey, and S. P. Tear, Phys. Rev. B **62**, 5016 (2000).
[35] T. J. Wood, C. Bonet, T. C. Q. Noakes, P. Bailey, and S. P. Tear, Surf. Sci. **598**, 120 (2005).
[36] J. W. M. Frenken, J. F. van der Veen, and R. M. Tromp, Nucl. Instrum. Methods Phys. Res. B **17**, 334 (1986).